Int. J. Electrochem. Sci., 15 **(2020)** 2070 – 2088, doi: 10.20964/2020.03.66

International Journal of
ELECTROCHEMICAL
SCIENCE
www.electrochemsci.org

Ultratough and Reversibly Stretchable Zwitterionic poly(ionic liquid) Copolymer Hydrogel with High Ionic Conductivity for High-Performance Flexible and Cold-Resistant Supercapacitor

Ximan Bu[1], *Linlin Wu*[1,*], *Xiaofeng Ma*[2], *Wenjing Diao*[1], *Duyou Lu*[1,*]

[1] College of Materials Science and Engineering, Nanjing Tech University, Nanjing 210009, P. R. China
[2] College of Science, Nanjing Forestry University, Nanjing 210037, P. R. China
[*]E-mail: llwu@njtech.edu.cn; duyoulu@njtech.edu.cn

Received: 7 November 2019 / *Accepted:* 1 January 2020 / *Published:* 10 February 2020

It remains challenging to develop hydrogel electrolyte with integrated superior mechanical properties and ionic conductivity for high performance flexible supercapacitors. Herein, copolymer hydrogels are prepared *via* a one-step polymerization of acrylamide (AM), 3-(1-vinyl-3-imidazolio) propanesulfonate (VIPS) zwitterionic monomer and 3-sulfopropyl methacrylate potassium salt anionic monomer (SPMA). On one hand, the ionic interaction as reversible "sacrificial bonds" provided by VIPS and SPMA through SO_3^-—H_3N^+ makes these hydrogels tough (fracture energy 3.8 MJ m^{-3}), stretchable (fracture strain 5100%), flexible and self-recoverable (~98% recovery efficiency after 1000% strain deformed). On the other hand, high ionic conductivity (3.1 S m^{-1}) is achieved due to the efficient ion migration channels derived from the zwitterionic copolymer with high hydration capacity. Based on this hydrogel, the as-prepared flexible supercapacitor not only exhibits high discharge capacitance of 108.8 F g^{-1} at 1 A g^{-1}, and retains ~99% of its capacitance after 1000 cycles, but also achieves encouraging performance at subzero temperature due to the prevention of ice formation by zwitterionic polymer. This hydrogel can be easily functionalized with ionic liquid or other functional materials to extend their practical application.

Keywords: hydrogel; zwitterionic poly(ionic liquid); ionic conductivity; flexible supercapacitor

1. INTRODUCTION

Flexible supercapacitors (SCs) with high performance, such as mechanical stability and superior ionic conductivity, are highly desired to meet the growing demands of emerging flexible and wearable electronic devices [1-5]. Owing to their intrinsic flexibility, low cost, environmental security, and designable nature, hydrogel networks swollen by electrolyte solutions (*e.g.* NaCl and LiCl) have recently been explored as gel polymer electrolytes (GPEs) for flexible supercapacitors [6-9]. Typically,

ionic conductivity and mechanical robustness are considered as two important factors that will affect electrochemical performance and stability of supercapacitors. In recent years, various tough hydrogels were developed based on "sacrificial bonds" toughing mechanism [10-13], and ionic conductive hydrogel with additional functions (*e.g.* self-healable) were also prepared by introducing non-covalent interactions [14-17]. However, the inverse relationship between ionic conductivity and mechanical robustness has made it very challenging to develop stretchable polymer electrolytes with improved ionic conductivity for next-generation multifunctional high performance solid-state SCs.

Zwitterionic poly(ionic liquid) (PIL) hydrogel, a class of polyelectrolyte with both cation and anion covalently linked to the polymer backbone, has been demonstrated as potential GPEs material in energy storage devices due to their robust water retention ability and efficient ion migration channels [18-19]. Moreover, the zwitterionic groups may impart improved mechanical strength of hydrogel and can strengthen the adhesion between gel electrolyte and electrode interface through interchain electrostatic interaction/adhesion [18, 31-32]. For example, Peng et al. recently reported poly(propylsulfonate dimethylammonium propylmethacrylamide) zwitterionic hydrogel electrolyte (PPDP/LiCl) with high water retention ability and high ionic conductivity, which greatly increased the electrochemical performance of graphene-based solid-state supercapacitor [18]. More importantly, zwitterionic compounds can serve as extremely effective "dissociation enhancers" to enhance the dissociation degree of lithium ion from polyelectrolyte due to ion-dipole interactions thus greatly improve the conductivity of electrolyte materials [20]. Unfortunately, most of the zwitterionic hydrogels present low mechanical properties. Furthermore, though the conductivity of GPE can be improved, the addition of electrolyte salt into zwitterionic hydrogel will eliminate physical crosslinking formed by interchain electrostatic interaction thereby worsening mechanical performance [21]. In addition, zwitterionic polymer chains with high ionic species may strongly bond water and prevent the ice formation at subzero temperature, it is expected to achieve high-performance cold-resistant supercapacitor based on the zwitterionic hydrogel as GPEs. In a word, zwitterionic hydrogel with integrated tough, stretchable, cold-resistant and highly ionic conductive properties is highly desired for high performance flexible supercapacitors.

The dynamic ionic interaction between oppositely charged groups that can be established by polymerizing oppositely charged monomers, has the advantages of not only acting as reversible "sacrificial bonds" to toughen hydrogel, endow hydrogels with healable abilities [22-24], but also introducing counterions (along with high water retention) in charged polyelectrolyte thus enabling a high conductivity [25]. For example, highly flexible and healable polyampholyte (PA) hydrogel crosslinked by dynamic ionic interactions has a potential as GPEs with high ionic conductivities for supercapacitors and the SCs-PA-KOH shows excellent specific capacitance at low temperatures, such as −30 °C, owing to disrupted ice formation in the PA networks [26, 27]. Based on these studies, it is anticipated to alter the mechanical properties and ionic conductivity of zwitterionic hydrogels *via* copolymerizes with polyelectrolyte possessing anionic or cationic functionalities by forming ionic interaction [28, 29]. In this way, zwitterionic hydrogel with integrated stretchable and high intrinsic ionic conductivity without doping electrolyte can be achieved in virtue of the electrostatic interaction, ion loading and ion migration channel derived from the synergistic effect of the highly charged zwitterionic polyelectrolyte copolymer for flexible supercapacitors.

Herein, a multifunctional hybrid crosslinked zwitterionic hydrogel of poly(acrylamide-co-3-(1-vinyl-3-imidazolio) propanesulfonate-co-3-sulfopropyl methacrylate potassium) P(AM-VIPS-SPMA) was prepared *via* a one-step copolymerization. VIPS/SPMA provides the resultant hydrogels with high mechanical performance (tensile strength of 126 kPa and stretchability of 5100%) and excellent ionic conductivity (3.1 S m^{-1}). The high-density dynamic ionic interactions between cationic group of VIPS and negatively charged SPMA offer additional physical crosslinking which makes the hydrogel tough, flexible and recoverable. The synergistic effect of the high ion loading and efficient ion migration channels deriving from the highly charged zwitterionic polyelectrolyte copolymer, makes the hydrogel highly ionic conductive. The above merits ensure this hydrogel attractive as ideal gel electrolyte for high-performance supercapacitors. The SCs based on this hydrogel not only exhibits high discharge capacitance of 108.8 F g^{-1} at 1 A g^{-1}, and retains ~99% of its capacitance over 1000 cycles, but also achieves encouraging performance at subzero temperature due to the disrupted ice formation by zwitterionic polymer.

2. EXPERIMENTAL

2.1. Materials

Acrylamide (AM, 99%), 3-sulfopropyl methacrylate potassium salt (SPMA, 96%), N, N′-methylene bisacrylamide (MBA, 99%) and 2-Hydroxy-4′-(2-hydroxyethoxy)-2-methylpropiophenone (photo-initiator) were purchased from Aladdin reagent (Shanghai, China). All the reagents were used without further purification. Deionized water was used through the experiments.

2.2. Synthesis of VIPS zwitterionic ionic liquid monomer

The compound 1-Vinylimidazole (6.3 g, 0.067 mol) was dissolved in 80 mL acetone. Then, an equimolar amount of 1,3-propanesultone (8.2 g, 0.067 mol) in 40 mL acetone was slowly added to the above solution at 0 ºC under a nitrogen atmosphere. The reaction mixture was then stirred for 5 days at room temperature. The obtained solid product was washed with acetone and then dried under vacuum at room temperature for 12 h. The purity of the product was confirmed by ^{1}H NMR (600 MHz) in D_2O: 8.975 (1H, s), 7.668 (1H, d), 7.506 (1H, d), 6.984 (1H, q), 5.656 (1H, d), 5.290 (1H, d), 4.297 (2H, t), 2.832 (2H, t), 2.230 (2H, m).

2.3. Preparation of P(AM-VIPS-SPMA) zwitterionic hydrogel

The zwitterionic PIL copolymer hydrogel was prepared by a simple one-step method. AM, MBA, SPMA, VIPS and the photo-initiator were added into water in a tube. The solution was stirred till all the reactants was dissolved and mixed homogeneously. Then the solution was degassed for three times and injected into a glass mold. At last, the solution in the glass mold was photo-polymerized using UV light (365 nm) for 1 h to form a zwitterionic PIL copolymer hydrogel. Zwitterionic PIL copolymer hydrogel with VIPS/SPMA in equimolar and totally 10%, 20% and 30% in hydrogel were

prepared. For control tests, PAM hydrogel without SPMA/VIPS were synthesized using the same experiment process. All samples with various compositions are listed in Table 1.

Table 1. Composition of various hydrogels

Sample	AM (wt%)	VIPS/SPMA (wt%)	MBA (μL, 10 mg ml^{-1})	UV-initiator (g)
PAM	20	0	80	0.0379
P(AM-VIPS-SPMA)	20	10	90	0.0437
P(AM-VIPS-SPMA)	20	20	102	0.0495
P(AM-VIPS-SPMA)	20	30	114	0.0553

2.4. Characterization

The hydrogel film with thickness of 1 mm was dried at 50 °C until all water was removed. The FTIR-ATR absorption spectra of the dried films were recorded using a Nicolet Nexus 670 spectrometer in the range of 4000–600 cm^{-1}. The average size distribution of the aggregates in the PVIPS and SPMA aqueous solutions was measured by Dynamic Light Scattering (DLS) method (Malvern Instruments Ltd., Malvern, UK). The laser light-scattering angle was set to 90°. The morphologies of the freeze-dried hydrogels were identified using FEI Quanta 200 scanning electron microscope (SEM). The gel was refrigerated for 48 h and then placed in a freeze dryer for 24 h at -60 °C. The freeze-dried samples were broken in liquid nitrogen, and the obtained sections were sprayed with gold. ^{1}H NMR spectra were measured using a 600 MHz AVANCE III HD instrument (Bruker).

The mechanical performances of all hydrogel samples were measured by an electromechanical universal testing machine (CMT2103). The tensile tests of gel samples (5.5 mm in diameter; standard distance 10 mm) were measured at a tensile speed of 100 mm min^{-1}. The compressive mechanical properties of gel samples (22 mm in diameter; height 10 mm) were evaluated at a crosshead speed of 20 mm min^{-1}. The fracture energy is calculated by the area contained in the stress-strain curve.

Ionic conductivity was measured in a blocking-type cell where hydrogel membranes were sandwiched between two stainless steel electrodes by the electrochemical impedance spectroscopy (EIS) method. The impedance measurements were taken under an electrochemical working station CHI660E (Chenhua, Shanghai) in the frequency range of 0.01 Hz to 100 kHz with an open circuit potential mode using AC excitation voltage of 5 mV at room temperature. The ionic conductivity of hydrogels can be calculated from Eq. (1) from the known area and thickness of hydrogel membranes:

$$\sigma_{\mathrm{H}} = \frac{l}{R_{\mathrm{b}}\mathrm{A}} \qquad (1)$$

Where l is the hydrogel membrane thickness (cm), A is the activity area (cm^2) and R_b is the resistance of the hydrogel membrane.

2.5. Fabrication and Electrochemical Performance of SCs

The SCs were fabricated by sandwiching the zwitterionic PIL hydrogel between two electrodes as shown in Fig. 3. The electrodes used in SCs are self-made activated carbon electrodes. Activated carbon (TF-B520 type, Shanghai Sinotech Co. Ltd) was grinded into powder, then activated carbon, acetylene black (Alfa Aesar) and PVDF binder (Solvay-1030 type, Solvay Solexis Co. Ltd) was mixed together in 8:1:1 mass ratio. A required amount of NMP was added into the mixed powder with constant stirring to form slurry, followed by agitating in an ultrasonic water bath for 30 min for a better dispersion. After that, the slurry was coated on two carbon cloths (10×25 mm) and the carbon cloths were dried at 80 ºC for 12 h. Zwitterionic PIL hydrogel simultaneously served as separator and electrolyte was sandwiched between the two symmetrical self-made activated carbon electrodes.

The electrochemical performance of SCs was tested in a two-electrode system. The cyclic voltammetry (CV) and galvanostatic charge–discharge (GCD) data were measured by the CHI 660E electrochemical workstation (Chenhua, Shanghai) at different scan rates and current densities. The cycling stability of SCs was performed with a sweep charge and discharge rate at the current density of 2 A g^{-1} for 1000 cycles.

The discharge specific capacity of the supercapacitor can be calculated from the galvanostatic charge-discharge curves:

$$C_{SP} = \frac{I\Delta t}{m\Delta V} \quad (2)$$

Where C_{sp} is the supercapacitor specific capacitance, I is the discharge current, Δt is the discharge time, m is the total mass of activated carbon on the two electrodes, respectively, ΔV is voltage change.

Also, the energy density and power density are calculated according to the following equations:

$$E = \frac{Csp\Delta V^2}{2} \quad (3)$$

$$P = \frac{E}{\Delta t} \quad (4)$$

Where E is the energy density, C_{SP} is the specific capacitance calculated from equation (2), ΔV is the voltage change, P is power density and Δt is the discharge time.

3. RESULTS AND DISCUSSION

3.1. Design Strategy and Characterization of Zwitterionic PIL Copolymer Hydrogel

The synthesis process and formation mechanism of P(AM-VIPS-SPMA) zwitterionic PIL hydrogel are illustrated in Fig. 1. 1-vinylimidazole was first quaternized with 1, 3-propane sulfonate to yield 3-(1-vinyl-3-imidazolio) propanesulfonate (VIPS) zwitterionic monomer and subsequently polymerized with AM monomer and SPMA anionic monomer in the presence of a small amount of

MBA chemical crosslinker in aqueous solution by photopolymerization. The introduction of VIPS and SPMA can provide additional high-density dynamic ionic interaction in the form of SO_3^-—H_3N^+ in the resulting hydrogel and work as sacrificial bonds to toughen hydrogel and endow the self-recovery ability to the resulting hydrogel [22]. Moreover, ionic conductivity of hydrogel can also be greatly increased due to the enhanced transport of oppositely K^+ counterions of SPMA polyelectrolyte in ion migration channels formed along the zwitterionic polyelectrolyte chains, thus making the multifunctional zwitterionic PIL hydrogel itself without doping salt as a single ion conducting GPE material for flexible energy devices [29].

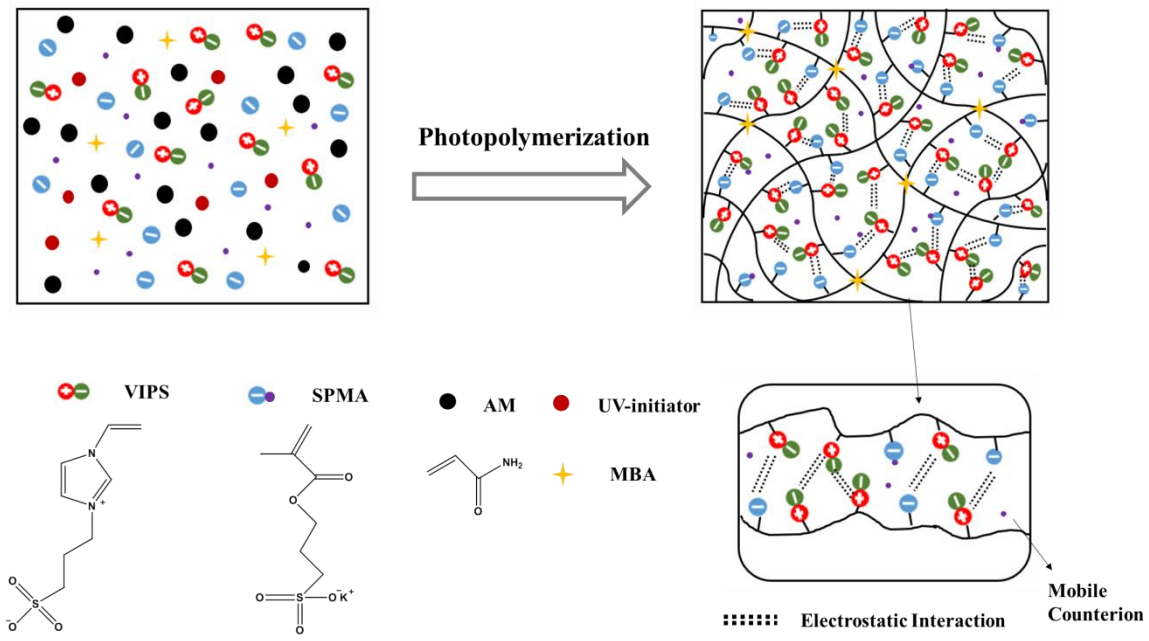

Figure 1. Schematic fabrication of P(AM-VIPS-SPMA) zwitterionic PIL hydrogels.

The successful synthesis of VIPS monomer is verified by ^{1}H NMR (Fig. S1). Fig. S2a shows the FTIR spectra of SPMA, VIPS, PAM gels and P(AM-VIPS-SPMA) gels. For PAM gel, the characteristic absorption bands at 3336 cm^{-1} and 3172 cm^{-1} represent a stretching vibration of N–H. The bands at 1628 cm^{-1} of C=O stretching, 1598 cm^{-1} of N–H deformation for primary amine, and C–N stretching for primary amide at 1414 $cm^{-1}$of the PAM or MBA in the gel system were also detected. For P(AM-VIPS-SPMA) gels, the absorption peaks at 1042 cm^{-1} associated with the symmetric stretching adsorption peaks of S=O and the peaks at 1165 cm^{-1} attributed to the asymmetric S=O absorption were detected, which indicates the appearance of SPMA and VIPS moiety. The characteristic absorption peak of the carbon skeleton on the benzene ring appears at 1451 cm^{-1}. These characteristic adsorption peaks confirm that P(AM-VIPS-SPMA) gels were successfully synthesized. The ionic interaction between VIPS and SPMA was confirmed by DLS characterization. As shown in Fig. S2b, DLS data of PVIPS solution in presence of different concentrations of SPMA was recorded. The DLS data revealed that, PVIPS (2 wt%) in aqueous solution formed aggregates of ~258 nm size. In presence of SPMA the average size gradually increased up to ~1400 nm. The increased size of

microdomain originates from the ionic complexation of PVIPS and SPMA monomer [28]. Moreover, as observed by SEM in Fig. S2c and d, compared to the pore structure of the PAM gel, P(AM-VIPS-SPMA) zwitterionic hydrogel exhibits a more dense network structure with significantly reduced pore size, which indicates the increased crosslinking degree by the additional high density dynamic SO_3^-—H_3N^+ ionic interaction.

3.2. Stretchability and toughness of zwitterionic PIL copolymer hydrogels

Mechanical properties are critical parameters of hydrogels for their practical applications in solid-state SCs. Fig. 2a shows representative tensile stress–strain curves of P(AM-VIPS-SPMA) zwitterionic hydrogels with various VIPS/SPMA concentration (from 0% to 30%). The tensile strength increased from 62 kPa (0%), 70 kPa (10%), 95kPa (20%), to 126 kPa (30%), whereas the fracture strain increased from 4676% to 5100% with VIPS/SPMA increased from 10% to 30%. The simultaneously increased tensile strength and fracture strain with the increase of VIPS/SPMA is presumably due to the electrostatic interactions provided by VIPS and SPMA [30-31]. Thus, the corresponding toughness of the zwitterionic PIL copolymer hydrogels was highly enhanced with increase of VIPS/SPMA concentration (Fig. 2b). The highest toughness (3.8 MJ m^{-3}) of P(AM-VIPS-SPMA) zwitterionic hydrogel is 1.7 times higher than that of pure PAM hydrogel (2.3 MJ m^{-3}). Besides, the corresponding compression strength is remarkably improved from 0.32 MPa (0%), 0.61 MPa (10%), 0.76 MPa (20%), to 1.34 MPa (30%) at the strain of 80% (Fig. 2c). The mechanical robustness of zwitterionic PIL hydrogels is also demonstrated in Fig. 2d and it can resist highly stretching, twisted stretching, stretching each other and bear 1000 g weight without any observable damage. The enhanced mechanical properties of P(AM-VIPS-SPMA) zwitterionic hydrogels (Table S1) with the increase of VIPS/SPMA concentration is believed to stem from electrostatic interactions exist between the cationic groups of VIPS and negatively charged SPMA and hydrogen bonding among PAM chains in the network [31, 32]. Electrostatic interaction not only results in a more compact network structure but also serves as new “sacrificial bonds” that greatly toughen the zwitterionic PIL hydrogels [22, 23]. The high toughness of zwitterionic PIL copolymer hydrogels was also illustrated in cyclic tensile properties and the corresponding dissipated energy is highly enhanced with increase of VIPS/SPMA concentration (Fig. S3a). The highest dissipated energy of P(AM-VIPS-SPMA) zwitterionic hydrogel (30%) at 1000% strain (737.4 kJ m^{-3}) is 2.1 times higher than that of PAM hydrogel (349 kJ m^{-3}) (Fig. S3a and b), which was attributed to the unzipping of hydrogen bond among PAM and electrostatic interactions within VIPS and SPMA in the network. Additionally, it can be seen from Fig. S3c and d that the dissipated energy of P(AM-VIPS-SPMA) zwitterionic hydrogel (30%) increased from 363.3 kJ m^{-3} at 500% strain to 1985 kJ m^{-3} at 2000% strain. This phenomenon further indicates that more hydrogen bonding and electrostatic interactions in zwitterionic PIL hydrogel break at larger strain deformation.

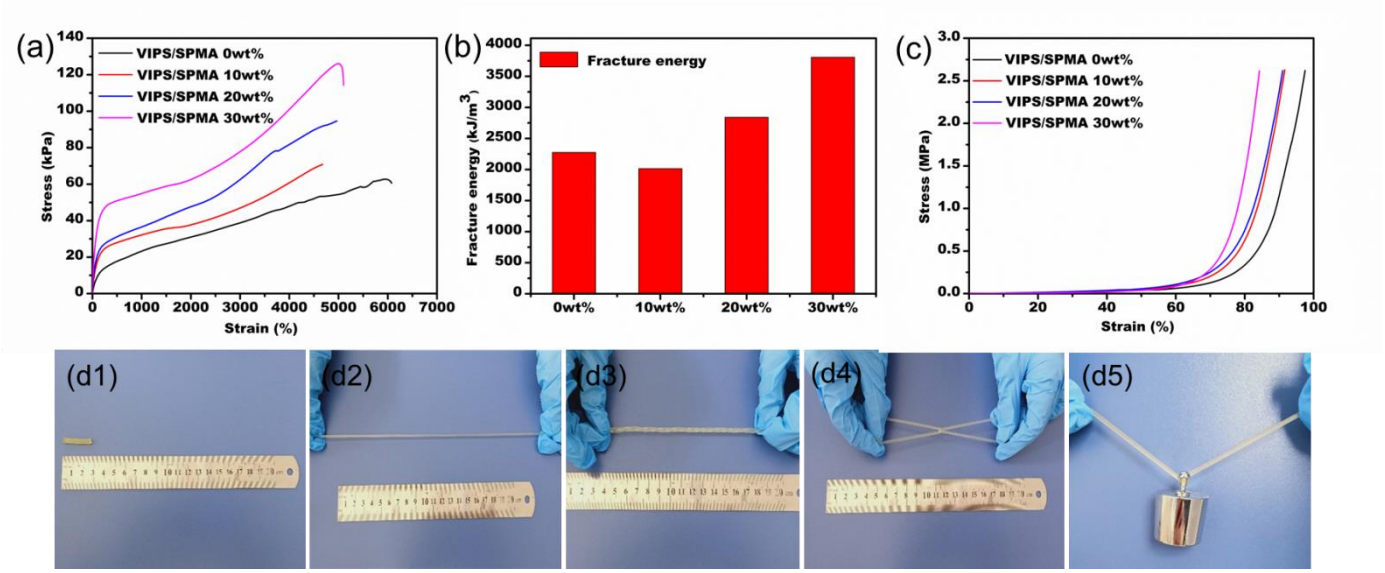

Figure 2. (a) Tensile stress–strain curves, (b) the corresponding fracture energy, and (c) compression stress–strain curves of P(AM-VIPS-SPMA) zwitterionic PIL hydrogels at different VIPS/SPMA concentrations. Zwitterionic PIL hydrogels withstand different high-level deformations of (d1 and d2) stretching, (d3) twisted stretching, (d4) stretching each other, and (d5) a small cylindrical zwitterionic PIL hydrogel bearing 1000 g weight.

3.3. Reversible high stretchability of zwitterionic PIL hydrogels under fatigue damage

Tough hydrogels that can rapidly recovered after being heavily fatigue damaged is very important for the further development of reversibly stretching supercapacitor devices. In order to further study the fatigue resistant properties of zwitterionic PIL copolymer hydrogels, eight successive tensile loading tests of P(AM-VIPS-SPMA) zwitterionic hydrogel (30%) were performed at a very large (1000%) strain deformation. As shown in Fig. S4a and b, the hysteresis loops and energy dissipation of P(AM-VIPS-SPMA) zwitterionic hydrogel were the largest (751 kJ m^{-3}) in the first tensile loading cycle. However, the hysteresis loops and elastic moduli appeared obvious decrease in the following tensile loading cycles. The decreased energy dissipation and elastic modulus after the first loading cycle suggests a significant softening in the zwitterionic copolymer hydrogel under such large tensile strain deformation. Successive cyclic tensile loading tests on the same P(AM-VIPS-SPMA) zwitterionic hydrogel (30%) at various strain ranging from 500% to 2000% without resting were also performed (Fig. 3a). It can be found that elastic modulus of the zwitterionic hydrogel decreased from 70 kPa at 500% strain to 13 kPa at 2000% strain. Moreover, the defined softness parameter calculated according to the equation, $(1 - E_x/E_0) \times 100$, where E_x and E_0 are elastic moduli at x and initial modulus, increased to 20% at 500% strain and to 84% at 2000% strain (Fig. 3b) [33]. These results illustrate that the zwitterionic PIL copolymer hydrogel with chemical (MBA chemical crosslinking) and physical (hydrogen bonding and ionic interaction) hybrid crosslinking do suffer from fatigue damage due to the internal fracture of gel network with large 1000% strain deformation and the damage could not be recovered without resting [34].

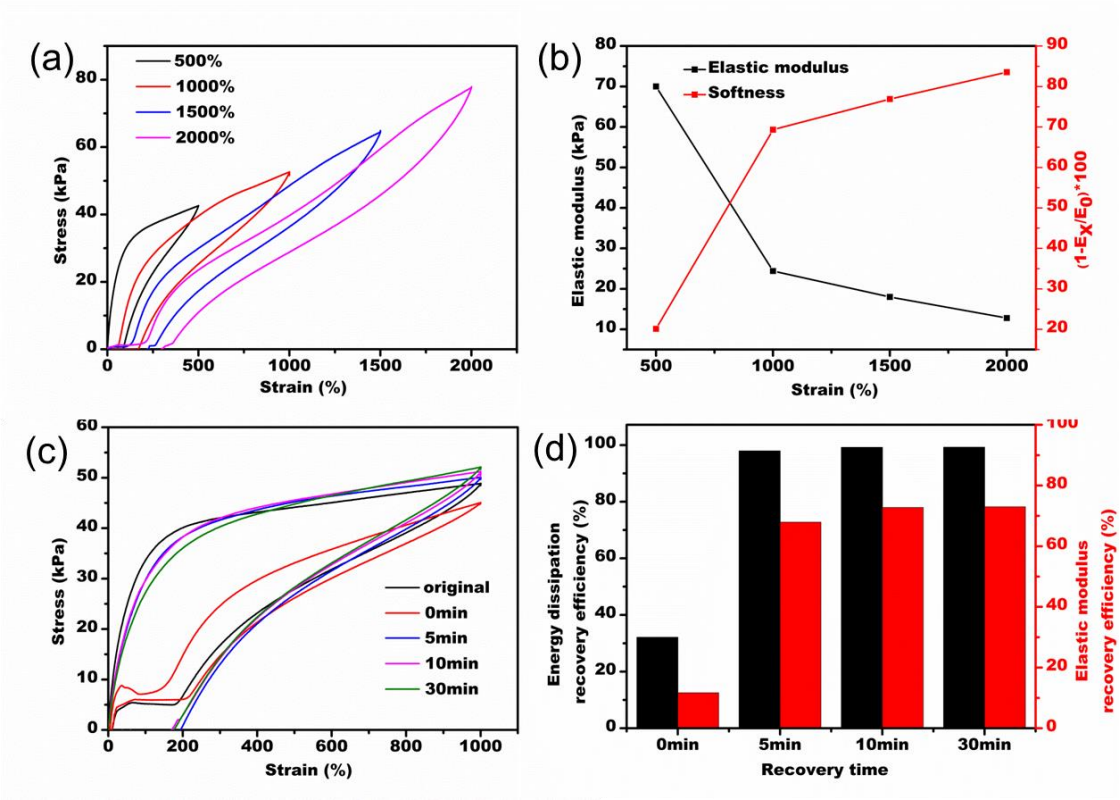

Figure 3. (a) Successive loading-unloading curves of the same P(AM-VIPS-SPMA) (30 wt%) zwitterionic hydrogel at different increased strain without resting between any two consecutive loadings and (b) Elastic modulus and softness of zwitterionic PIL hydrogel (30 wt%) at different strain. (c) Self-recovery of zwitterionic PIL hydrogel (30 wt%) at different resting times at room temperature and (d) the corresponding energy dissipation and elastic modulus recovery rates.

Self-recovery property of P(AM-VIPS-SPMA) zwitterionic hydrogel can be expected due to the exist of the reversible intermolecular hydrogen bonds and electrostatic interactions between the cationic groups of VIPS and negatively charged SPMA, which can be induced at room temperature with enough healing time. It can be seen from Fig. 3c that stress–strain curves can gradually recover to the original loading pathway with increased resting time at 1000% strain. The toughness recovers to 67% and 97%, whereas stiffness recovers to 72% and 98% of original hydrogel after resting for 5 and 10 min, respectively (Fig. 3d). The results indicate that zwitterionic PIL copolymer hydrogels possess very excellent self-recovery properties, which is mainly ascribed to the dynamic electrostatic interaction and hydrogen bonding that reconstitute the fracture network, thereby facilitating the recovery of hydrogel. The excellent self-recovery performance of zwitterionic PIL hydrogels guarantees the durability of the hydrogel for further development of reversibly stretching supercapacitor devices.

3.4. Ionic conductivity and application of zwitterionic hydrogel as electrolyte in flexible solid-state SCs

Ionic conductivity of P(AM-VIPS-SPMA) zwitterionic hydrogel has great influence on the electrochemical performance of supercapacitors. As shown in Fig. 4, two LEDs were successfully

lightened by P(AM-VIPS-SPMA) zwitterionic hydrogel served as the conductor. The ionic conductivity of P(AM-VIPS-SPMA) zwitterionic hydrogels increases with the VIPS/SPMA concentration from 0.46 S m^{-1} (10%), 0.93 S m^{-1} (20%) to 3.1 S m^{-1} (30%), which is much higher than the conductivity of lithium copolymer polyzwitterion (0.056 S m^{-1}) [29]. The enhanced ionic conductivity benefits from the increased ion loading and efficient ion migration channel derived from the synergistic effect of the highly charged zwitterionic polyelectrolyte copolymer. Interestingly, the ionic conductivity and mechanical strength of hydrogels can be enhanced simultaneously with the increasing of VIPS/SPMA concentration. These features break away the intrinsic conflict between good mechanical properties and high ionic conductivity of GPEs.

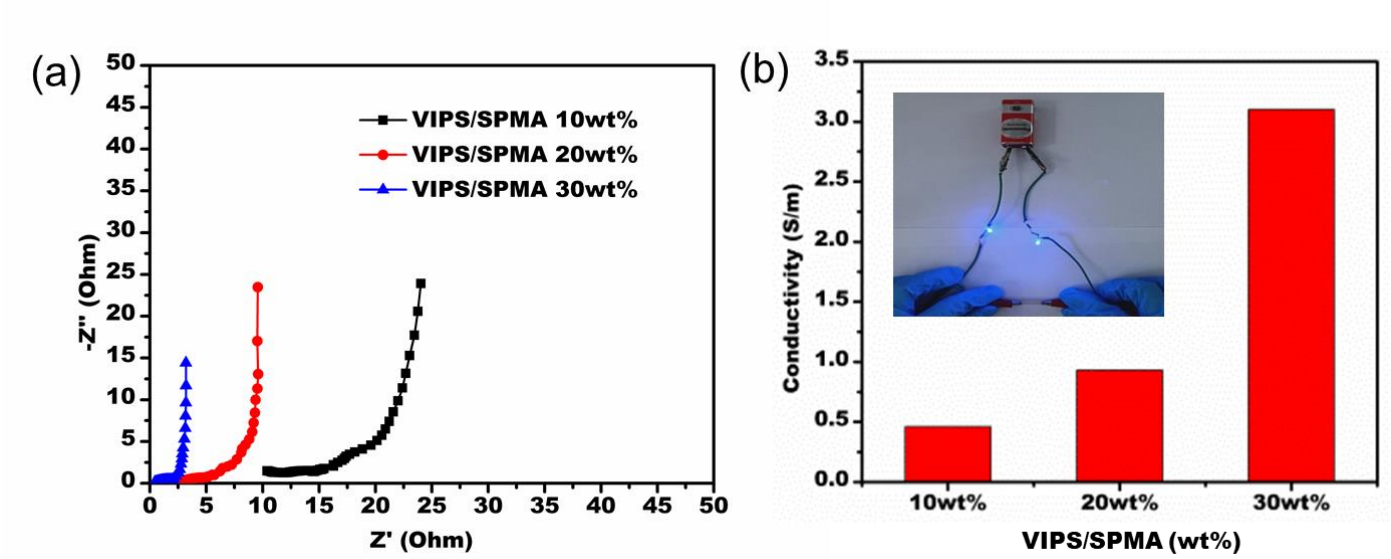

Figure 4. (a) Electrochemical impedance spectra and (b) ionic conductivity of P(AM-VIPS-SPMA) zwitterionic hydrogel with different VIPS/SPMA concentration at 25 °C.

Such zwitterionic PIL hydrogels with excellent mechanical properties and ionic conductivity are ideal GPEs for flexible energy storage devices. As an example of application, the obtained P(AM-VIPS-SPMA) zwitterionic hydrogel was used to assemble a flexible supercapacitor. The supercapacitor was assembled by sandwiching a piece of P(AM-VIPS-SPMA) (30%) zwitterionic hydrogel between two activated-carbon/carbon-cloth electrodes (Fig. 5a). The electrochemical performances of the P(AM-VIPS-SPMA) zwitterionic hydrogel based SCs were investigated. The galvanostatic charge–discharge (GCD) and cyclic voltammetry (CV) curves with different cut-off voltages were used to identify a suitable operating voltage. As shown in Fig. 5b, the GCD curves at 2 $A \cdot g^{-1}$ approximates an isosceles triangle when the cut-off is lower than 0.8 V. Similarly, the same conclusion was reached from the CV analysis (Fig. 5c). As expected, the CV curves of supercapacitor between 0 and 0.8 V at the scan rates of 5–50 mV s^{-1} displayed rectangular shape (Fig. 5d), indicating a remarkable rate capability. In addition, all isosceles triangle-shaped GCD profiles at different current densities ranging from 1 to 6 A g^{-1} are shown in Fig. 5e, exhibiting a typical reversible double layer capacitive behavior.

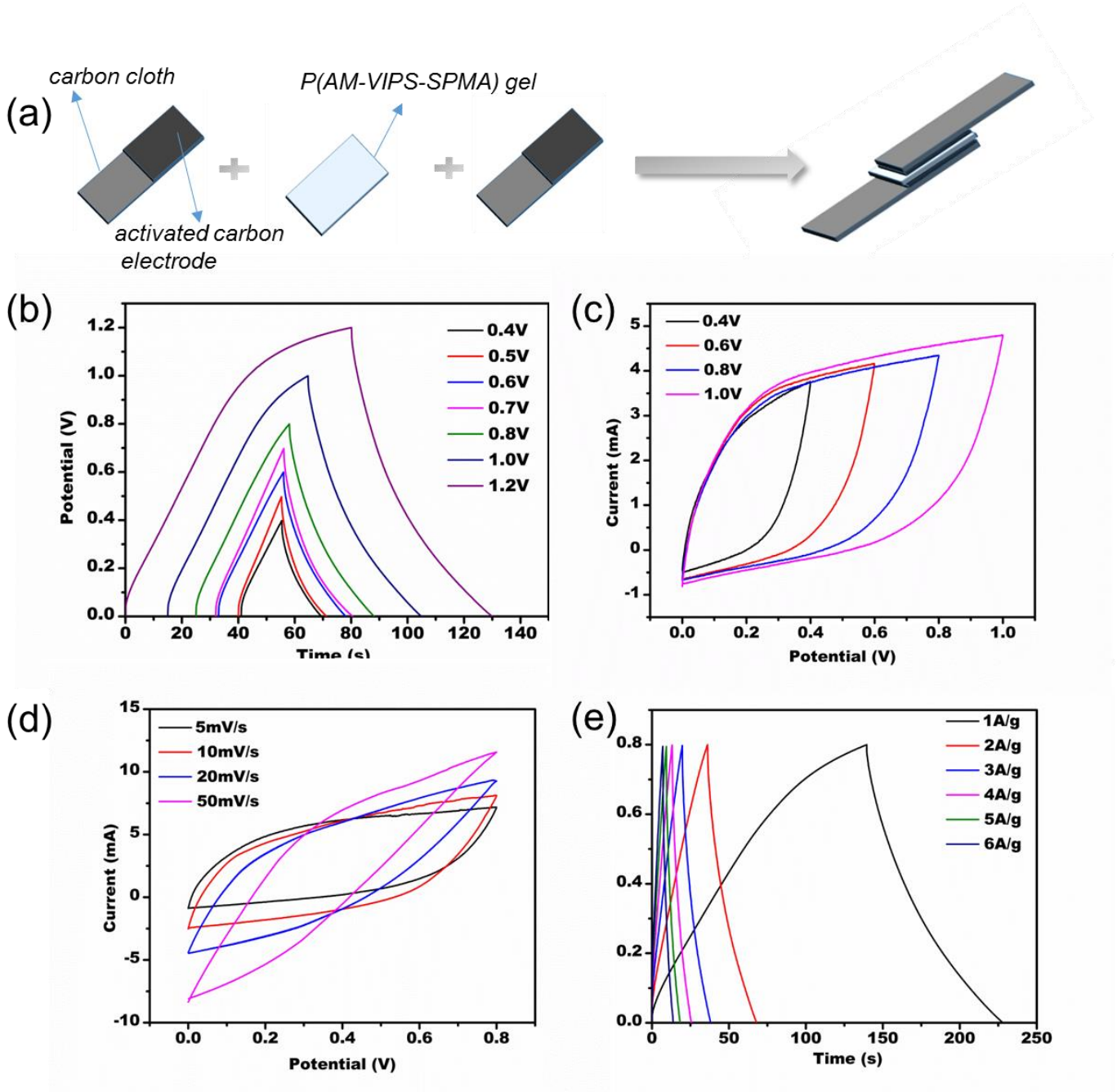

Figure 5. (a) Schematic illustration of the fabrication process of SC–P(AM-VIPS-SPMA) based flexible symmetric supercapacitor. Electrochemical performances of SCs–P(AM-VIPS-SPMA): (b) GCD curves at various cut-off voltages at a current density of 2 A g^{-1}; (c) CV curves at various cut-off voltages at a scan rate of 5 mV s^{-1}; (d) CV curves at various scan rates; (e) GCD curves at various current density.

A non-polyelectrolyte PAM hydrogel (VIPS/SPMA, 0 wt%) based flexible supercapacitor was also assembled and the electrochemical performances of SC–P(AM-VIPS-SPMA) was compared with SC–PAM. SC–P(AM-VIPS-SPMA) possesses much lower internal resistance (1.04 Ω) compared with SC–PAM (6.14 Ω) (Fig. 6a), which could be mainly ascribed to the highly conductive P(AM-VIPS-SPMA) copolymer with high ionic load, ion dissociation and transport [20, 29]. The charged groups in polyelectrolyte copolymer also greatly increase the interface adhesion between the zwitterionic

copolymer hydrogel and electrodes, thereby greatly enhance the conductivity of the whole device. Correspondingly, SC–P(AM-VIPS-SPMA) exhibited much better performance and its discharge capacitance (108.8 F g^{-1}) is roughly 3.3 times that of the SC-PAM (33.7 F g^{-1}) at 1 A·g^{-1} (Fig. 6b and c). Meanwhile, the SC–P(AM-VIPS-SPMA) maintained satisfactory performance at a higher current density benefiting from the low internal resistance. The as-fabricated supercapacitor applying P(AM-VIPS-SPMA) gel electrolyte exhibited better rate capacity, with only 44% capacitance loss when the current density increased from 1 to 4 A·g^{-1}compared with 92% loss for the as-fabricated supercapacitor applying PAM gel. Furthermore, SC–P(AM-VIPS-SPMA) could even operate at a current density of 6 A·g^{-1} with 52% capacitance loss. Moreover, as shown in Fig. 6d, SC-P(AM-VIS-SPMA) show a higher energy density and power density compared to the SC-PAM. The energy density of SC–P(AM-VIPS-SPMA) was 9.67 Wh/kg at a power density of 400 W/kg, which is about 3.1 times than that of SC–PAM (3.1 Wh/kg). And the performance of SC-P(AM-VIS-SPMA) was superior to those of similar previously reported devices using hydrogel electrolyte as listed in Table 2. Therefore, the zwitterionic poly(ionic liquid) gel based flexible supercapacitor exhibit both excellent capacitance and rate capacity, which is derived from the synergizes effects of robust water retention ability and the ion migration channel with high ionic conductivity built by the hydration layer along with the polyelectrolyte copolymer chains and the electrostatic adhesion between interfaces [18, 29].

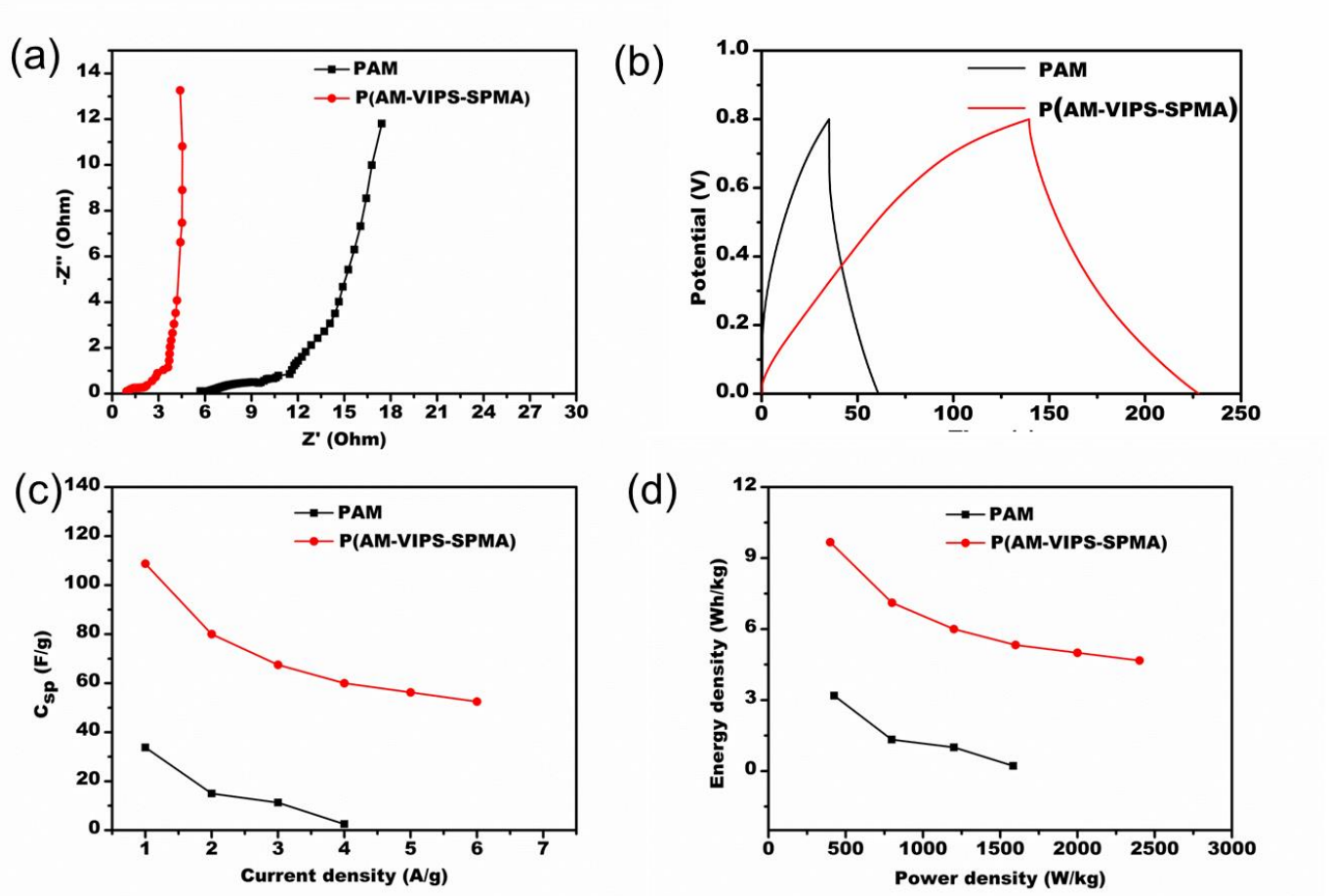

Figure 6. Electrochemical performances of supercapacitors fabricated with different GPEs, i.e., PAM and P(AM-VIPS-SPMA) gel: (a) Nyquist plots, (b) GCD profiles at 1 A g^{-1}, (c) the specific capacity at various current densities and (d) Ragone plots.

Table 2. Comparison of mechanical behavior and capacitor performances with different hydrogel electrolyte.

Hydrogel electrolyte	Electrode	Strain (%)	Stress (kPa)	Potential (V)	Capacitance	Refs.
PAMPSA/PVA/LiCl	PPy@SWCNTs	938	112.6	0.8	297 mF cm^{-2}at 0.5 mA cm^{-2}	[35]
P(AA-*co*-AAm)/$CoCl_2$	AC	1200	600	1	134.1 Fg^{-1}at 0.5 A g^{-1}	[36]
PVA-*g*-TMAC/KCl	AC	600	30	1	89.0 F g^{-1} at 1 A g^{-1}	[37]
KCl–Fe^{3+}/PAA	GF@PPy	700	400	1	85.4 F g^{-1} at 1 A g^{-1}	[8]
PAD/H_2SO_4	PANI	2900	1800	0.6	430 mF cm^{-2} at 0.5 mA cm^{-2}	[38]
Agar/HPAAm	PPy	3400	750	0.6	138.3 mF cm^{-2} at 0.2 mA cm^{-2}	[39]
SA-g-DA/KCl	AC	310	4.2	1	93 F g^{-1} at 0.5 A g^{-1}	[17]
P(AM-VIPS-SPMA)	AC	5100	126	0.8	108.8 F g^{-1} at 1 A g^{-1}	This work

Cycling performance is a crucial characteristic for evaluating the stability of solid-state supercapacitors based on P(AM-VIPS-SPMA) zwitterionic hydrogel. At a high current density of 2 A g^{-1}, capacitance retention of ~99% was obtained after 1000 successive GCD cycles (Fig. 7). Additionally, the columbic efficiency of SC–P(AM-VIPS-SPMA) was maintained at about 88%. The excellent cycling performance of the as-assembled SCs is largely attributed to the long-term stability of P(AM-VIPS-SPMA) zwitterionic hydrogel. The excellent electrochemical performances make the new P(AM-VIPS-SPMA) zwitterionic gel attractive for fabricating the next generation of solid-state supercapacitors.

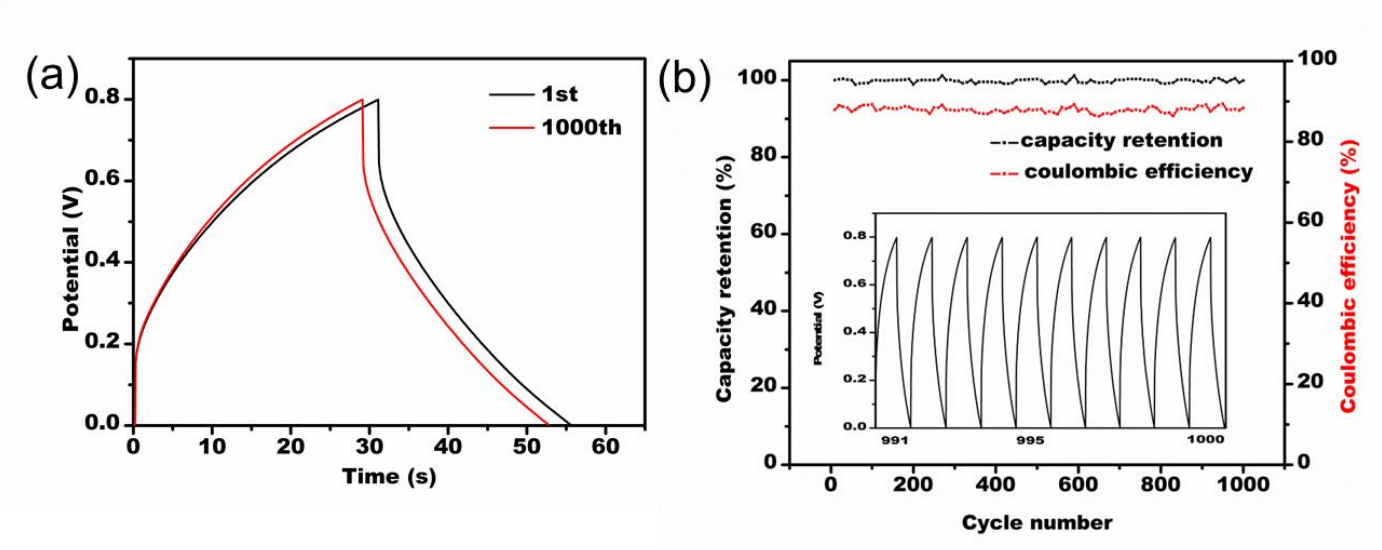

Figure 7. Cycling performance of SC–P(AM-VIPS-SPMA). (a) The 1st cycle and 1000th cycle of GCD curves at 2 A g^{-1} and (b) cycling stability under 1000 cycles at 2 A g^{-1}.

The electrochemical performances of SCs–P(AM-VIPS-SPMA) at low temperatures is also very important for their practical applications. Interestingly, the SCs–P(AM-VIPS-SPMA) demonstrate good capacitive performances between 0 °C and −10 °C. Fig. 8a shows the Nyquist plot of the SC–P(AM-VIPS-SPMA) at different temperatures. The equivalent series resistance of SC–P(AM-VIPS-SPMA) was 1.93 Ω and 2.95 Ω at 0 °C and −10 °C, respectively. As shown in Fig. 8b and c, the supercapacitor also shows quasi-rectangle shaped CVs and triangular GCD profiles at the temperature range, suggesting a stable electrochemical performance and a low electrical resistance of the whole device. Its specific capacitance are 38.75 F g^{-1} at 0 °C and 15 F g^{-1} at −10 °C, which are 36% and 15% of those measured at room temperature (25 °C), respectively (Fig. 8d). It should be note that such performance of SCs was achieved by applying P(AM-VIPS-SPMA) zwitterionic PIL copolymer hydrogel without other electrolyte. The performances are believed to arise from the high conduction of the zwitterionic PIL copolymer hydrogel at −10 °C due to the strongly bound water on ionic species of P(AM-VIPS-SPMA) zwitterionic copolymer chains which cannot participate in ice formation [18]. To our knowledge, very few hydrogel electrolytes based capacitors exhibited the low temperature capacitive behaviors derived from the special polymer structure [26]. The feature allows zwitterionic PIL hydrogel having potential application for solid-state capacitors operating at low temperature.

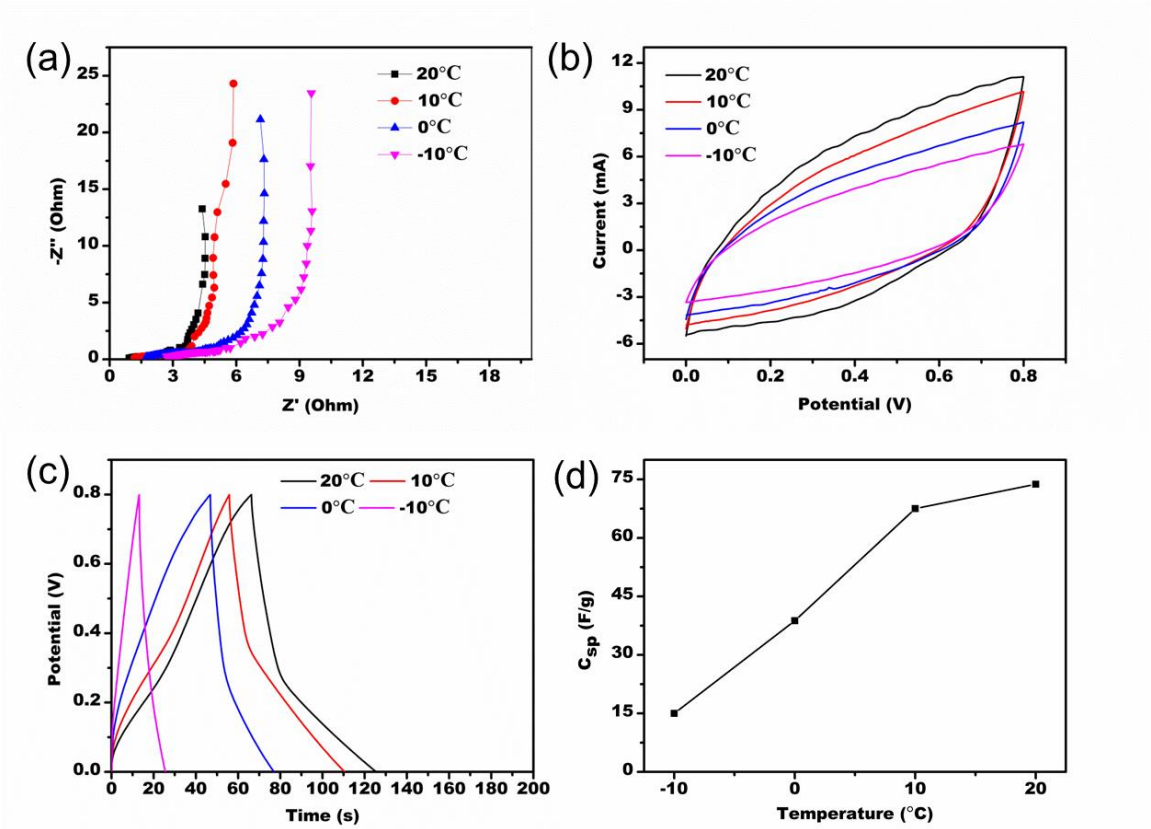

Figure 8. Electrochemical performances of the SCs–P(AM-VIPS-SPMA) at low temperatures: (a) the Nyquist plots, (b) CVs at 50 mV s^{-1} and (c) GCD profiles at different temperatures at 1 A g^{-1} and (d) calculated specific capacitance at various temperature.

4. CONCLUSIONS

Tough and highly ionic conductive P(AM-VIPS-SPMA) zwitterionic poly(ionic liquid) copolymer hydrogel comprising high density dynamic ionic interactions between VIPS and SPMA was successfully fabricated. The simultaneously excellent mechanical strength and ionic conductivity are achieved in virtue of the electrostatic interaction, high ion loading and efficient ion migration channel derived from the charged groups of poly(ionic liquid) copolymer. The as-synthesized P(AM-VIPS-SPMA) zwitterionic copolymer hydrogel shows a high tensile strength of 126 kPa, fracture strain of 5100%, toughness of 3.8 MJ m^{-3} and can obtain 98% recovery efficiency after 1000% strain deformation. The P(AM-VIPS-SPMA) based supercapacitor delivers a high discharge capacitance of 108.8 F g^{-1} at 1 A g^{-1} and can retention ~99% of its capacitance after 1000 cycles, due to the highly ionic conductive P(AM-VIPS-SPMA) poly (ionic liquid) and the electrostatic adhesion between electrode and GPE interfaces. Furthermore, a supercapacitor based on this hydrogel without doped salt as gel electrolyte also achieves encouraging performance at subzero temperature, owing to the prevention of ice formation by zwitterionic polymer with high ionic species. Therefore, the designed flexible zwitterionic hydrogel with integrated enhanced mechanical strength and electrochemical properties is a promising candidate for applications in next-generation flexible wearable devices.

ACKNOWLEDGMENTS
This work was supported by the Natural Science Foundation of Jiangsu Province (BK20160992).

APPENDIX A. SUPPLEMENTARY DATA
Supplementary data to this article can be found online at https://doi.org/10.1016/j.jpowsour.

References

1. L. B. Hu, M. Pasta, F. La Mantia, L. F. Cui, S. Jeong, H. D. Deshazer, J. W. Choi, S. M. Han, Y. Cui, *Nano Lett.,* 10(2010) 708.
2. C. Larson, B. Peele, S. Li, S. Robinson, M. Totaro, L. Beccai, B. Mazzolai, R. Shepherd, *Science,* 351(2016) 1071.
3. C. C. Kim, H. H. Lee, K. H. Oh, J. Y. Sun, *Science,* 353(2016) 682.
4. Z. T. Zhang, J. Deng, X. Y. Li, Z. B. Yang, S. S. He, X. L. Chen, G. Z. Guan, J. Ren, H. S. Peng, *Adv. Mater.,* 27(2015) 356.
5. L. Kou, T. Q. Huang, B. N. Zheng, Y. Han, X. L. Zhao, K. Gopalsamy, H. Y. Sun, C. Gao, *Nat. Commun.,* 5(2014) 3754.
6. Y. Huang, M. Zhong, F. Shi, X. Liu, Z. Tang, Y. Wang, Y. Huang, H. Hou, X. Xie, C. Zhi *Angew. Chem., Int. Ed.,* 56(2017) 9141.
7. Y. Huang, M. Zhong, Y. Huang, M. S. Zhu, Z. X. Pei, Z. F. Wang, Q. Xue, X. M. Xie, C. Y. Zhi, *Nat. Commun.,* 6(2015) 10310.
8. Y. Guo, X. Zhou, Q. Tang, H. Bao, G. Wang, P. Saha, *J. Mater. Chem. A,* 4(2016) 8769.
9. H. Li, T. Lv, N. Li, Y. Yao, K. Liu, T. Chen, *Nanoscale,* 9(2017) 18474.
10. P. Lin, S. Ma, X. Wang, F. Zhou, *Adv. Mater.,* 27(2015) 2054.
11. Q. Chen, L. Zhu, C. Zhao, Q. Wang, J. Zheng, *Adv. Mater.,* 25(2013) 4171.
12. J. Y. Sun, X. Zhao, W. R. K. Illeperuma, O. Chaudhuri, K. H. Oh, D. J. Mooney, J. J. Vlassak, Z. Suo, *Nature,* 489(2012) 133.
13. X. Zhao, *Soft Matter,* 10(2014) 672.

14. Z. Wang, F. Tao, Q. Pan, *J. Mater. Chem. A,* 4(2016) 17732.
15. F. Tao, L. M. Qin, Z. K. Wang, Q. M. Pan, *ACS Appl. Mater. Interfaces,* 9(2017) 15541.
16. X. H. Liu, Z. B. Wen, D. B. Wu, H. L. Wang, J. H. Yang, Q. G. Wang, *J. Mater. Chem. A,* 2(2014) 11569.
17. T. Lin, M.Shi, F. Huang, J. Peng, Q. Bai, J. Li, M. Zhai, *ACS Appl. Mater. Interfaces,* 10(2018) 29684.
18. X. Peng, H. Liu, Q. Yin, J. Wu, P. Chen, G. Zhang, G. Liu, C. Wu, Y. Xie, *Nat. commun.,* 7(2016) 11782.
19. C. J. Lee, H. Wu, Y. Hu, M. Young, H. Wang, D. Lynch, F. Xu, H. Cong, G. Cheng, *ACS Appl.Mater. Interfaces,* 10(2018) 5845.
20. N. Byrne, J. M. Pringle, C. Tiyapiboonchaiya, D. R. MacFarlane, M. Forsyth, *Electrochim. Acta,* 50(2005) 2733.
21. H. Charaya, X. Li, N. Jen, H. J. Chung, *Langmuir,* 5(2019) 1526.
22. A.B. Ihsan, T. L. Sun, T. Kurokawa, S.N. Karobi, T. Nakajima, T. Nonoyama, C. K. Roy, F. Luo, J. P. Gong, *Macromolecules,* 49(2016) 4245.
23. F. Luo, T. L. Sun, T. Nakajima, T. Kurokawa, Y. Zhao, A. B. Ihsan, H. L. Guo, X. F. Li, J. P. Gong, *Macromolecules,* 47(2014) 6037.
24. F. Luo, T. L. Sun, T. Nakajima, T. Kurokawa, Y. Zhao, K. Sato, A. B. Ihsan, X. Li, H. Guo, J. P. Gong, *Adv. Mater.,* 27(2015) 2722.
25. T. Long, Y. Li, X. Fang, J. Sun, *Adv. Funct. Mater.,* 28(2018) 1804416.
26. X. Li, L. Liu, X. Wang, Y. S. Ok, J. A. Elliott, S. X. Chang, H. J. Chung, *Sci. Rep.,* 7(2017) 1685.
27. J. Wei, C. Yin, H. Wang, Q. Wang, *J. Mater. Chem. A,* 6(2017) 58.
28. S. Mandal, N. Pandey, S. Singh, A. Ranjan, U. Ojha, *Mater. Chem. Front.,* 3(2019) 690.
29. C. Tiyapiboonchaiya, J. M. Pringle, J. Sun, N. Byrne, P. C. Howlett, D. R. MacFarlane, M.Forsyth, *Nat. Mater.,* 3(2004) 29.
30. Z. Lei and P. Wu, *Nat. Commun.,* 9(2018) 1134.
31. W. Diao, L. Wu , X. Ma, Z. Zhuang, S. Li, X. Bu, Y. Fang. *J. Appl. Polym. Sci.,* 136(2019) 47783.
32. H. Liu, C. Xiong, Z. Tao, Y. Fan, X. Tang, H. Yang, *RSC Adv.,* 5(2015) 33083.
33. Q. Chen, X. Yan, L. Zhu, H. Chen, B. Jiang, D. Wei, L. Huang, J. Yang, B. Liu, J. Zheng, *Chem. Mater.,* 28(2016) 5710.
34. Z. Tang, F. Chen, Q. Chen, L. Zhu, X. Yan, H. Chen, B. Ren, J. Yang, Q. Gang, J. Zheng*, Polym. Chem.,* 8(2017) 4659.
35. B. Zhang, J. Li, F. Liu, T. Wang, Y. Wang, R. Xuan, G. Zhang, R. Sun, C.P. Wong, *Chem. - A Eur. J.,* 25(2019) 11715.
36. L. Dai, W. Zhang, L. Sun, X. Wang, W. Jiang, Z. Zhu, H. Zhang, C. Yang, J. Tang, *ChemElectroChem,* 6(2019) 467.
37. Z. Wang, Q. Pan, *Adv. Funct. Mater.,* 27(2017) 1700690.
38. Y. Shi, Y. Zhang, L. Jia, Q. Zhang, X. Xu, *ACS Appl. Mater. Interfaces,* 10(2018) 36028.
39. Y. Wang, F. Chen, Z. Liu, Z. Tang, C. Zhi, *Angew. Chem., Int. Ed.*,58(2019) 15707.

SUPPORTING INFORMATION

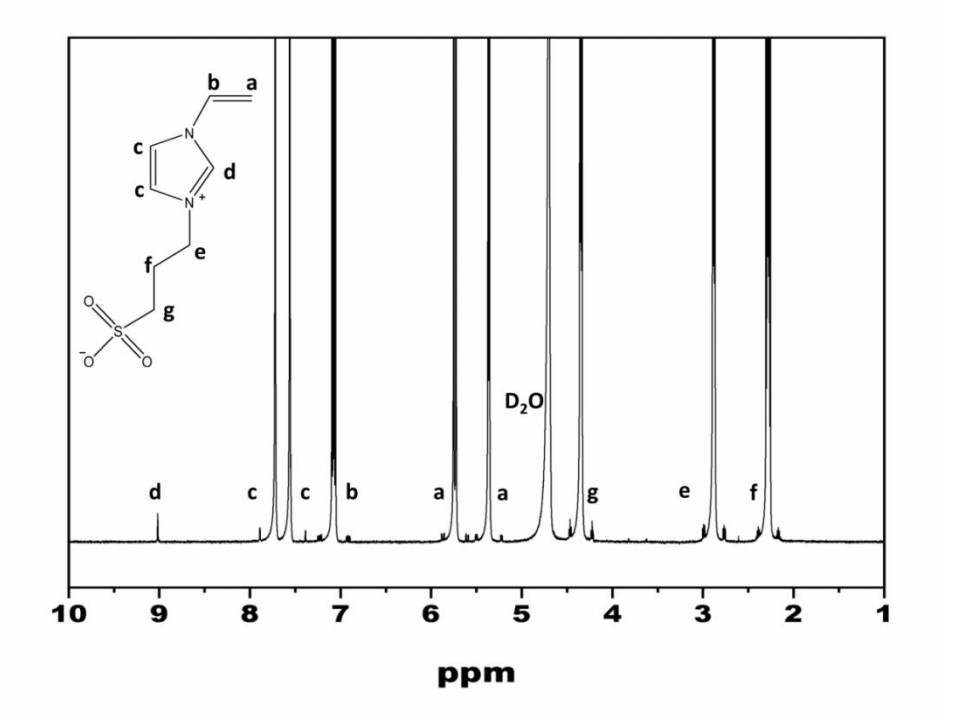

Figure S1. ^{1}H NMR spectra of VIPS in D_2O.

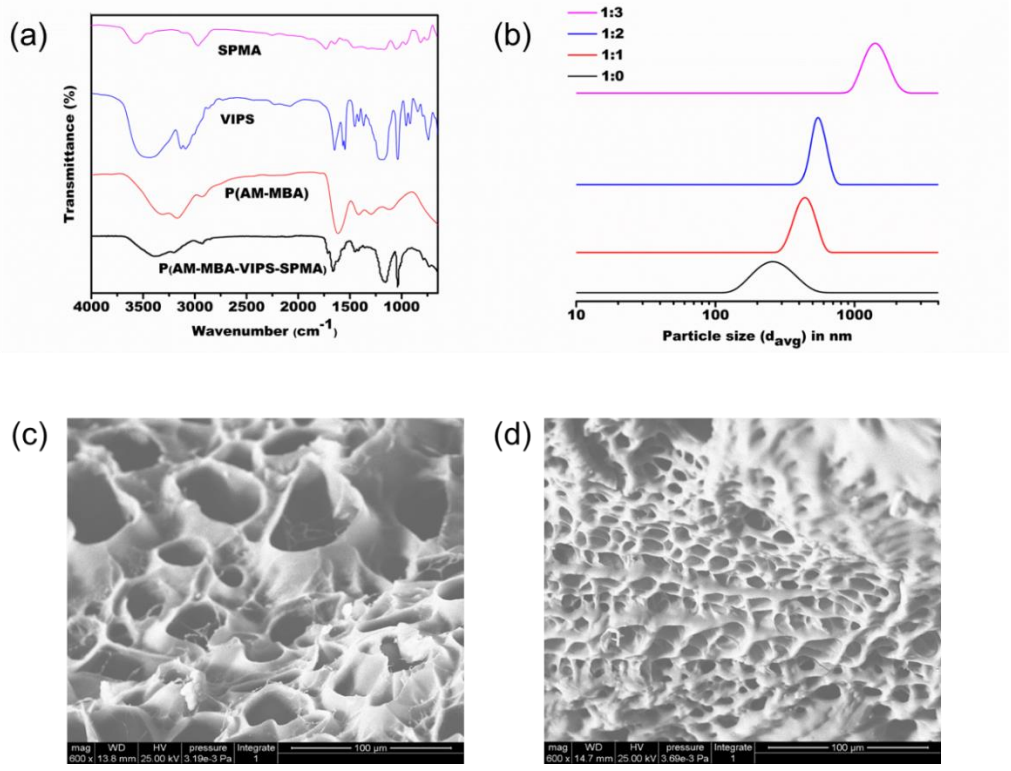

Figure S2. (a) FTIR-ATR analysis of SPMA, VIPS, PAM gel and P(AM-VIPS-SPMA) gel, (b) DLS traces of aqueous PVIPS (2 wt% solution) and effect of incremental addition of SPMA, SEM images of (c) PAM gel and (d) P(AM-VIPS-SPMA) gel.

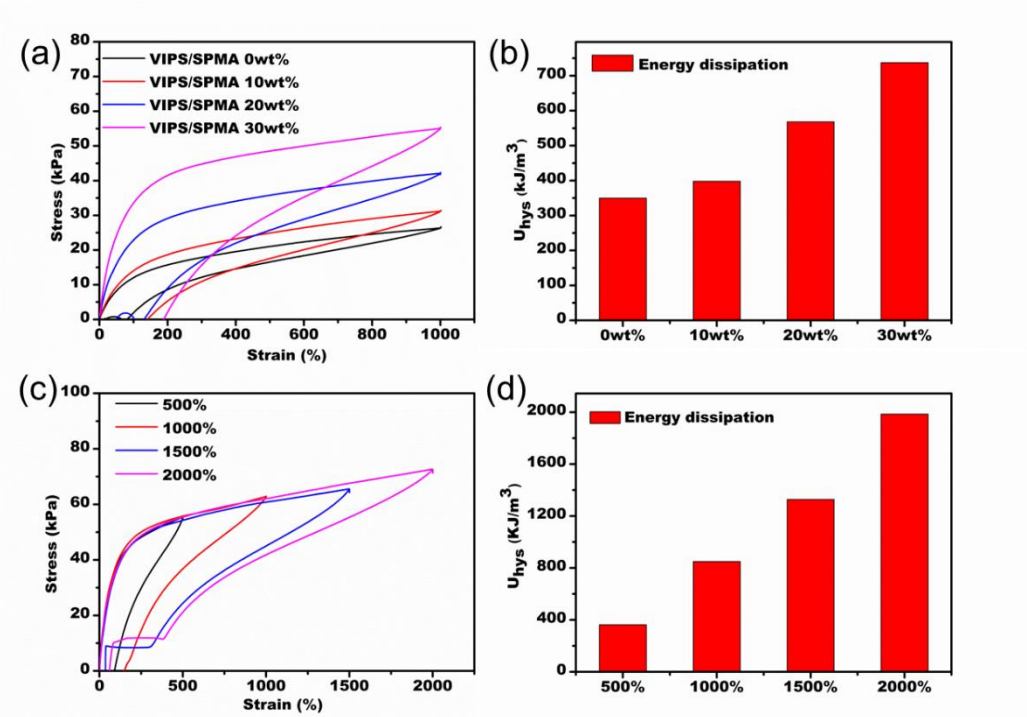

Figure S3. (a) Cyclic loading-unloading curves at 1000% strain and (b) the corresponding dissipated energy (Uhys) of the P(AM-VIPS-SPMA) gels at different VIPS/SPMA concentrations. (c) Cyclic loading curves and (d) the corresponding dissipated energy of P(AM-VIPS-SPMA) gels (VIPS/SPMA 30 wt%) at different maximum strain.

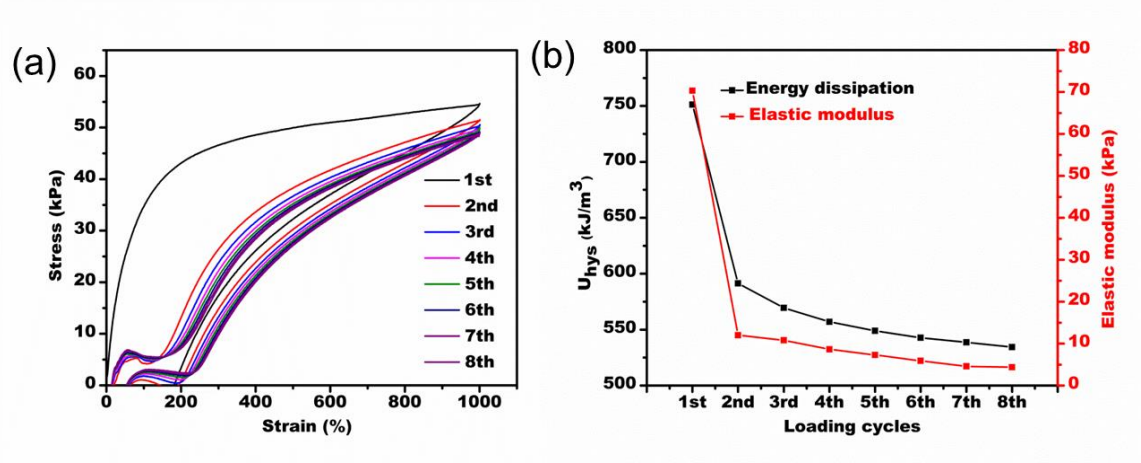

Figure S4. (a) Successive loading-unloading curves of the same P(AM-VIPS-SPMA) gel (30 wt%) at 1000% strain. No resting time is applied between any two consecutive loadings. (b) Elastic modulus and softness of P(AM-VIPS-SPMA) gels at 1000% strain.

Table S1. Mechanical properties of different hydrogels

VIPS-SPMA (%)	Fracture strain (%)	Tensile strength (kPa)	Toughness (MJ m^{-3})	Compression strength (MPa)
0	6073	62	2.3	0.32

10	4267	70	2.1	0.61
20	4931	95	2.8	0.76
30	5100	126	3.8	1.34